Lab on a Chip

Cite this: *Lab Chip*, 2012, **12**, 3798–3802

www.rsc.org/loc

PAPER

Liquid sensing capability of rolled-up tubular optical microcavities: a theoretical study†

Fangyuan Zhao,[a] Tianrong Zhan,[b] Gaoshan Huang,[c] Yongfeng Mei*[c] and Xinhua Hu*[a]

Received 10th April 2012, Accepted 18th July 2012
DOI: 10.1039/c2lc40743d

Rolled-up tubular optical microcavities are a novel type of optical sensor for identifying different liquids and monitoring single cells. Based on a Mie scattering method, we systematically study the optical resonances and liquid sensing capability of microtubes. Analytical formulas are presented to calculate the resonant wavelengths λ_r, Q factors, sensitivities S and figures of merit QS. Both ideal and rolled-up microtubes are considered for different optical materials in tube walls (refractive indices ranging from 1.5 to 2.5) and for three setups: tube-in-liquid, hollow-tube-in-liquid and liquid-in-tube. It is found that for rolled-up microtubes, the highest QS can be achieved by using the liquid-in-tube setup and very thin wall thicknesses. A maximal sensitivity is found in the case of the liquid cylinder. Our theory well explains a recent experiment under the setup of tube-in-liquid. It is also found that, although it describes the case of tube-in-liquid well, the waveguide approximation approach is not suitable for the case of liquid-in-tube. The results could be useful to design better optofluidic devices based on rolled-up microtubes.

Introduction

Optofluidics is an emerging research field that combines microfluidics and optics.[1,2] Although the idea of using fluids and optics has been applied in examples such as oil-immersion microscopes and liquid-crystal displays,[3,4] modern optofluidics aims at creating similar devices on a smaller scale comparable to wavelengths.[5,6] By introducing microfluids, the propagation of light can be manipulated in a small photonic circuit.[7–9] On the other hand, the refractive indices of liquids n_L can be deduced from the wavelength of optical modes.[10–13] As a result, important devices such as tunable photonic circuits and lab-on-a-chip for physical, chemical and biological analyses could be achieved based on optofluidics.[1,2]

Microtubes are interesting optofluidic devices that can carry liquids and support optical resonances with whispering gallery modes (WGMs).[14–31] The original microtubes are stretched silica capillaries that have relatively large sizes (with outer diameter h = 80–100 μm and wall thickness Δ = 2–4 μm). [14–16] Although the optical resonances of microtubes can be detected by coupling microtubes with optical fibers, the measurement system is still complex and resonances with high Q factors are difficult to observe.

Recently, a novel class of microtubes, which have smaller sizes (h = 1–10 μm and Δ = 50–200 nm) and versatile wall composition, have been fabricated by rolling up prestressed solid thin films.[17–29] By incorporating photoluminescent materials into the tube walls, the optical resonances of the rolled-up microtubes can be easily detected from photoluminescent spectra especially for high-Q modes.[23–27] Due to their subwavelength wall thickness, the microtubes have resonances sensitive to ambient refractive index and thus are suitable for identifying different liquids.[28] Since their diameters are comparable to the size of a single cell, the rolled-up microtubes can also be applied to capture and monitor single cells, promising high potential for lab-on-a-chip applications.[29,31]

Although some studies have been performed on liquid-sensing with rolled-up microtubes (under the tube-in-liquid setup), the greatest possible performance of such liquid sensors, and how to realize it, remain unknown. In this paper, we present a comprehensive theoretical study on the optical resonances and liquid-sensing capability of rolled-up microtubes. Rigorous formulas are presented to calculate the resonant wavelength λ_r, Q factors, sensitivities $S \equiv d\lambda_r/dn_L$ and figures of merit QS of microtubes. In order to identify liquids with refractive index n_L of around 1.33 (water), we consider both ideal and rolled-up microtubes with different materials in the tube walls (with refractive indices from 1.5 to 2.5) and under three setups: liquid-in-tube, hollow-tube-in-liquid and tube-in-liquid [see Fig. 1(d)–1(f)]. It is found that for certain materials and resonant modes in rolled-up microtubes, the highest QS can be obtained by using

[a]*Department of Materials Science, Key Laboratory of Micro and Nano Photonic Structures (Ministry of Education) and Laboratory of Advanced Materials, Fudan University, Shanghai, 200433, China. E-mail: huxh@fudan.edu.cn*
[b]*Department of Physics and Key Laboratory of Surface Physics, Fudan University, Shanghai, 200433, China*
[c]*Department of Materials Science, Fudan University, Shanghai, 200433, China. E-mail: yfm@fudan.edu.cn*
† Published as part of a themed issue on optofluidics.

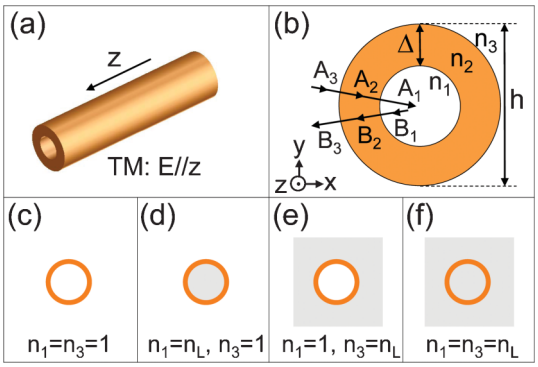

Fig. 1 (a) 3D and (b) cross-section schematic views of a microtube. The microtube has a diameter of h, wall thickness of Δ and refractive index of n_2 in the wall. The refractive indices are n_1 and n_3 for media inside and outside the microtube, respectively. The incident light is propagating in the x–y plane and has E field along the z direction. (c)–(f) The microtube is placed in four kinds of environment: in air (c), with liquid inside and air outside (d), with liquid outside and air inside (e) and in liquid (f). The liquid has a refractive index of n_L.

the liquid-in-tube setup and very thin wall thickness. A maximal sensitivity is found in the case of liquid cylinders. Based on our theory, a recent experiment is well explained and the applicability of a prevailing method of waveguide approximation is also identified.

Theory

The microtube under study has a two-layered cylindrical structure as shown in Fig. 1. The layer indices i are 1 and 3 for the media in and outside the microtube, respectively. $i = 2$ for the tube wall. The ith layer has an outer radius of r_i, refractive index of n_i and dielectric constant of $\varepsilon_i = n_i^2$. The microtube is along the z direction and perpendicular to the x–y plane. Transverse-magnetic/transverse-electric (TM/TE) resonances exist in microtubes and can be excited by TM/TE waves that propagate in the x–y plane and have the electric/magnetic field along the z direction. However, TM resonances have larger Q-factors than TE ones and thus are more suitable for sensing.[28,34] Hence, we focus on TM resonances, although formulas are presented for both TM and TE resonances.

Waveguide approximation

The wall of the microtube is a film with a refractive index of n_2. When this film is flat, it can support waveguide modes with propagating constants β satisfying

$$t_1 + t_3 - (1 - t_1 t_3)\tan(q_2 \Delta) = 0 \quad (1)$$

where $t_1 = \frac{q_1}{q_2}\left(\frac{\varepsilon_2 q_1}{\varepsilon_1 q_2}\right)$ and $t_3 = \frac{q_3}{q_2}\left(\frac{\varepsilon_3 q_1}{\varepsilon_1 q_3}\right)$ for waves with E (H) field parallel to the film, $q_1^2 = \beta^2 - n_1^2 k_0^2$, $q_3^2 = \beta^2 - n_3^2 k_0^2$, $q_2^2 = n_2^2 k_0^2 - \beta^2$, $k_0 = 2\pi/\lambda$, λ is the wavelength in vacuum, $n_1 = \sqrt{\varepsilon_1}$ and $n_3 = \sqrt{\varepsilon_3}$ are the refractive indices of media below and above the film, respectively.[28] Hence, WGM resonances occur in the microtube when

$$\beta L = 2\pi m \quad (2)$$

where $L = \pi (r_1 + r_2)$ and the integer m is the order of resonance.

Mie scattering method

Although the above waveguide method can be applied to estimate the resonant wavelengths of microtubes,[28,34] it cannot present Q factors and show the difference between the cases in Fig. 1(d) and 1(e). For rolled-up microtubes, the finite-difference time-domain (FDTD) method has been applied to obtain the Q factors and accurate values of λ_r.[20–22,24,25,27–29] However, the simulations are time consuming, especially for high-Q cases. Here, we apply a Mie scattering method to accurately obtain the resonant wavelengths and Q factors of microtubes.[32–35] When TM (TE) waves are incident on a microtube, the electric field E_z (magnetic field H_z) in the ith layer can be written as $\Sigma_m[a_{i,m}J_m(k_i r) + b_{i,m}H_m^{(1)}(k_i r)]e^{im\phi}$, where $k_i = n_i k_0$, and the Bessel function J_m and Hankel function of the first kind $H_m^{(1)}$ stand for incident and scattering waves, respectively. The cylindrical coordinates (r,ϕ) are in the x–y plane and have an origin at the center of the microtube. Using continuities of E_z (H_z) and $\frac{\partial E_z}{\partial r}$ ($\varepsilon^{-1}\frac{\partial H_z}{\partial r}$) for TM (TE) waves, we have

$$\frac{J_m'(u) + D_{i+1,m}H_m^{(1)'}(u)}{J_m(u) + D_{i+1,m}H_m^{(1)}(u)} = \frac{\alpha_i}{\alpha_{i+1}}\frac{J_m'(v) + D_{i,m}H_m^{(1)'}(v)}{J_m(v) + D_{i,m}H_m^{(1)}(v)} \quad (3)$$

where $u = k_{i+1}r_i$, $v = k_i r_i$, $D_{i,m} = b_{i,m}/a_{i,m}$ and $\alpha_i = k_i$ ($k_i\varepsilon_i$) for TM (TE) waves. Using $D_{1,m} = 0$ and eqn (2), we can obtain the scattering coefficient $D_{3,m}$ of the microtube. For plane-wave incidence, the total scattering cross section of the microtube is given by

$$C_s \equiv \sum_m C_{s,m} = \sum_m \frac{2\lambda}{\pi}|D_{3,m}|^2 \quad (4)$$

The partial scattering cross section $C_{s,m}$ with the mth order exhibits a Lorentz line shape near resonance, $C_{s,m} = p_m/[(k_0 - k_m)^2 + \gamma_m^2]$, where $k_m = 2\pi/\lambda_m$, λ_m is the resonant wavelength, γ_m is the damping rate and $p_m = 4k_0^{-1}\gamma_m^2$ when n_2 is real. We note that using three points of $C_{s,m}(k_0)$ near resonance, the resonant wavelength λ_m and quality factor $Q = k_m/(2\gamma_m)$ can be numerically obtained.

Results

Mode with $m = 40$

We first study the resonant mode with $m = 40$ for a microtube with $n_2 = 2$ and $\Delta = 0.02h$. Microtubes with such parameters can be fabricated by rolling up a SiO/SiO_2 film and following with a HfO_2 coated layer. Fig. 2(a) shows the partial scattering cross section $C_{s,40}$ for the microtube when it is immersed in water. From $C_{s,40}$, we can obtain the reduced resonant frequency h/λ_r of 8.14 for the TM resonance with $m = 40$. We note that Fig. 2(a) is valid for microtubes with different diameters h and the resonant wavelength λ_r is 675.7 nm for $h = 5.5$ μm. At the resonant wavelength, the electric field is found to be mainly concentrated in the tube wall as shown in Fig. 2(c) and 2(d). However, the fields of evanescent waves also enter the water since the thickness of the tube wall is much smaller than the resonant wavelength ($\Delta = 0.16\lambda_r$). From Fig. 2(b), we can see that the resonant

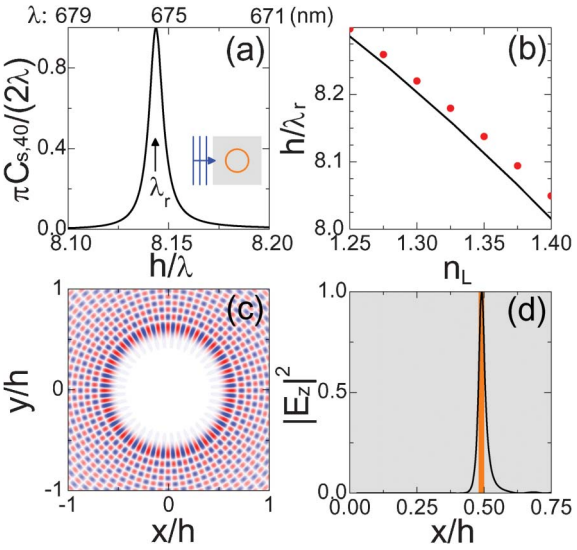

Fig. 2 (a) Partial scattering cross section with $m = 40$ for the microtube in Fig. 1(f). The parameters are $\Delta = 0.02h$, $n_2 = 2$ and $n_L = 1.33$ (water). For $h = 5.5$ μm, the scale of wavelength λ is shown on the top of (a). (b) The resonant wavelength λ_r in (a) as a function of n_L. The dots are approximated results from eqn (1) and (2). (c) Field Re (E_z) and (d) intensity $|E_z(x,y = 0)|^2$ for the resonant mode in (a). The blue, white and red colors in (c) represent positive, zero and negative, respectively. The gray and orange regions in (d) denote the water and tube wall, respectively.

wavelength can be well estimated by the waveguide approximation method. The resonant wavelength increases almost linearly with increasing refractive index of the liquid, giving rise to a sensitivity S of $0.3\lambda_r/n_L$ at $n_L = 1.33$. For the microtube with $h = 5.5$ μm, $S = 152$ nm/refractive index unit (RIU).

Fig. 3 shows the resonant and sensing parameters for microtubes with $n_2 = 2$, $m = 40$ and different wall thickness Δ. For microtubes with thick walls ($\Delta > 0.05h$), the resonant wavelengths of microtubes are found to have close values in different environments [see Fig. 3(a)]. However, the Q factors of microtubes strongly depend on the index n_3 of the outer medium [see Fig. 3(b)]. For microtubes with $\Delta > 0.01h$, the tube-in-liquid setup can present a higher sensitivity S than those found for the other two setups. But when $\Delta < 0.01h$, resonances exist only in the liquid-in-tube case. When Δ approaches zero, the liquid-in-tube case has $m\lambda_r/n_L \approx \pi h$ and thus can present the maximal sensitivity.

$$S_{max} = \lambda_r/n_L \quad (5)$$

In Fig. 3(a) and 3(b), the resonant wavelengths λ_r and sensitivities S are also calculated by the waveguide approximation method. It is found that for microtubes with $\Delta < 0.06h$ that are immersed in liquid, the waveguide approximation can present good estimation for both λ_r and S. However, this approximation method cannot show the difference between Fig. 1(d) and 1(e) and overestimates (underestimates) the sensitivity for the case of liquid-in-tube (hollow-tube-in-liquid).

The detection limit of sensing can be defined as $n_{DL} \equiv \lambda_{RS}/S$, where λ_{RS} is the sensor resolution.[14] Since 1/50 of the full width at half maximum (FWHM = λ_r/Q) of the resonant peak can be

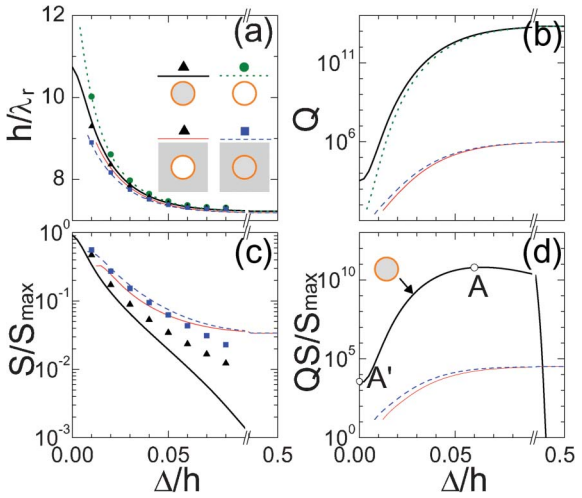

Fig. 3 (a) Wavelengths λ_r, (b) Q-factors, (c) sensitivities $S \equiv d\lambda_r/dn_L$ and (d) figures of merit QS for the $m = 40$ resonant modes of the microtubes in Fig. 1(d)–1(f). (a) and (b) also show the results for the microtube in Fig. 1(c). The parameters are $n_2 = 2$ and $n_L = 1.33$ (water). The symbols in (a) and (c) are approximated results from eqn (1) and (2).

used as λ_{RS}, we have $n_{DL} = \lambda_r/(50QS)$ so that QS can be regarded as the figure of merit for the liquid sensing with microtubes. For microtubes with $\Delta/h < 0.19$, the liquid-in-tube setup can present a higher QS than those found for the other two setups [see Fig. 3(d)]. Using the liquid-in-tube setup, an ideal microtube with $\Delta = 0.06h$ is found to possess the highest QS and thus the lowest detection limit.

The above studies are performed for ideal microtubes with quality factors of Q_i. For rolled-up microtubes, the quality factor $Q = (Q_i^{-1} + Q_s^{-1})^{-1}$ where Q_s is related to the loss from surface imperfection and cone effects ($Q < Q_i, Q_s$ and $Q_s < 5000$ for rolled-up microtubes). In Fig. 4, we simulate the imperfect microtubes phenomenologically by using a complex refractive index $n_2 = 2 + 0.004i$ in tube walls. It can be seen that although ideal and rolled-up microtubes have quite different Q factors, they exhibit almost the same resonant wavelengths and sensitivities. Here, the differences in λ_r and S between ideal

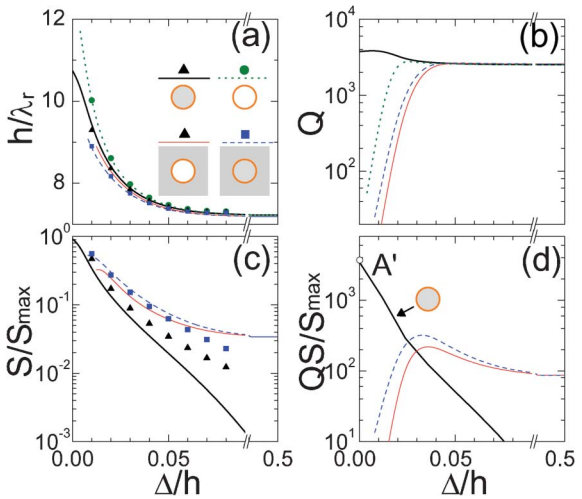

Fig. 4 As Fig. 3, but for microtubes with $n_2 = 2 + 0.0004i$.

and rolled-up microtubes are found to be about 0.0002. The reason is that adding a tiny imaginary part into the resonant frequency $f_r \propto 1/\lambda_r$ will not change $|f_r|$ and λ_r much, while it can lower the Q factor strongly ($Q = \mathrm{Re}(f_r)/\mathrm{Im}(f_r)$). The highest QS and lowest detection limit of $n_{DL} = 7.6 \times 10^{-6}$ RIU are found by the case of the liquid cylinder ($n_3 = 1$, $n_1 = n_L$ and Δ approaches 0).

By now we have shown that for ideal (rolled-up) microtubes with $n_2 = 2$, the highest QS and lowest detection limit can be achieved by using the liquid-in-tube setup and optimal wall thickness of $\Delta = 0.06h$ ($\Delta = 0$). Other nontoxic and transparent materials, which are usually oxides and have refractive indices n_2 ranging from 1.45 and 2.5, can be chosen in the tube walls. Fig. 5 shows the highest QS and corresponding parameters (Δ, λ_r, Q) for microtubes with $n_2 = 1.5$–2.5 and under the liquid-in-tube setup. For ideal microtubes, the optimal Δ increases from $0.05h$ to $0.07h$ with n_2 increasing from 1.5 to 2.5. As n_2 increases, the Q factor increases rapidly [see Fig. 5(b)] and the sensitivity decreases slightly [see Fig. 5(c)]. Hence, an ideal microtube with higher n_2 can present a higher QS and lower detection limit [see Fig. 5(d)]. However, for rolled-up microtubes with $Q < 5000$, the highest QS is achieved in the liquid-cylinder case and thus depends little on n_2.

Modes with m = 40–80

Oxides with defects such as SiO and HfO are usually incorporated into the walls of rolled-up microtubes and can show photoluminescent effects which facilitate the detection of WGM resonances of microtubes. For rolled-up microtubes with h = 5–10 μm, WGM resonances with m = 40–80 usually occur in the photoluminescent spectra (from 550 to 700 nm for SiO).

In Fig. 6, we show results for the resonances with orders m ranging from 40 to 80. Here, we focus on the case of $n_2 = 2$ and consider four different values of Δ/h and the two setups of tube-in-liquid and liquid-in-tube. The reduced resonant frequency h/λ_r is found to increase almost linearly with increasing m and the

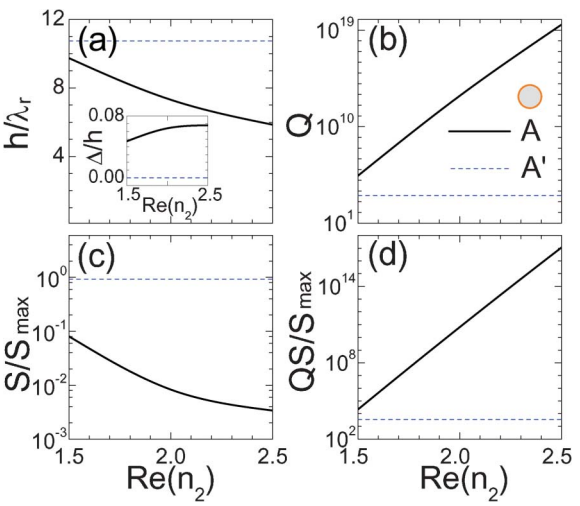

Fig. 5 (a) Resonant wavelengths λ_r, (b) Q-factors, (c) sensitivities S and (d) figures of merit QS of the optimal point A in Fig. 3(d) and A' in Fig. 4(d). Im (n_2) = 0 for A and Im (n_2) = 0.0002Re (n_2) for A'. The inset to (a) shows the wall thicknesses of microtube Δ at A and A'.

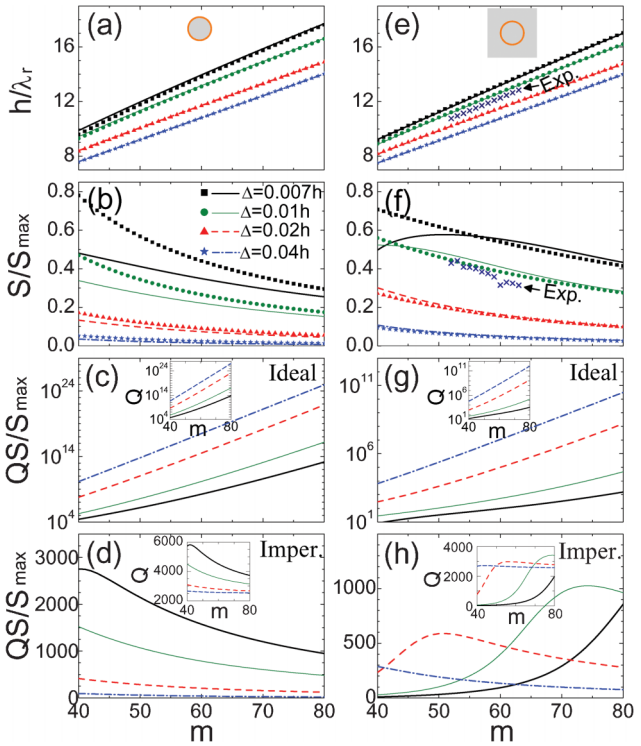

Fig. 6 Resonant wavelengths λ_r, sensitivities S, Q-factors and figures of merit QS as functions of order m for microtubes with Re (n_2) = 2. (a)–(d) and (e)–(h) are for the cases of Fig. 1(d) and 1(f), respectively. (c) and (g) are for ideal microtubes with Im (n_2) = 0. (d) and (h) are for imperfect microtubes with Im (n_2) = 0.0004. The symbols except crosses in (a), (b), (e) and (f) are approximated results from eqn (1) and (2). The crosses in (e) and (f) are experimental results for the microtube with h = 7 μm in Ref. 28.

curves can be well described by the waveguide approximation [see Fig. 6(a) and 6(e)]. From Fig. 6(b) and 6(f), it can be seen that the sensitivity S is found to mainly decrease with increasing the order m. Although the approximation method can well describe the case of tube-in-liquid, it cannot satisfactorily estimate the case of liquid-in-tube. Similar discrepancies between the approximated and accurate results can also be found in Fig. 3(c).

For ideal microtubes, the Q factor increases rapidly with increasing m so that the figure of merit QS also increases [see Fig. 6(c) and 6(g)]. However, for imperfect rolled-up microtubes in liquid, the Q factor increases with increasing m and approaches a constant value [see Fig. 6(h)]. Thus the highest QS is found at m = 75 (50) for rolled-up microtubes with $\Delta = 0.01h$ ($0.02h$) in liquid. For rolled-up microtubes with liquid inside, the Q factor decreases with increasing m so that the highest QS occurs at m = 40 [see Fig. 6(h)].

Comparison with experiments

In Fig. 6(e) and 6(f), we also plot recent experimental data for a rolled-up microtube with h = 7 μm.[28] It is found that the experimental result is very close to our theoretical case with $n = 2$ and $\Delta = 0.01h$. In previous experiments on rolled-up microtubes for liquid sensing, the tube-in-liquid setup is usually applied.[28] By comparing Fig. 6(d) and 6(h), we can see that if a scheme of

liquid-in-tube is used, the figure of merit will be improved three-fold for liquid sensing. We note that for the case of liquid-in-tube, the waveguide approximation fails and accurate methods such as the Mie scattering theory should be applied.

Conclusions

The optical resonances and liquid sensing capability of rolled-up microtubes have been studied systematically based on a Mie scattering method. Analytical formulas are presented to calculate the resonant wavelength λ_r, Q factor, sensitivity S and figures of merit QS. It is found that the highest QS can be achieved by using the liquid-in-tube setup and rolled-up microtubes with very thin wall thicknesses. Using this liquid-in-tube scheme, the figure of merit is predicted to be improved at least 3-fold over the current value with the tube-in-liquid setup. A maximal sensitivity is found in the case of the liquid cylinder. Our theory also well explains a recent experiment under the tube-in-liquid setup. It is also found that, although it describes well the case of tube-in-liquid, the approach of waveguide approximation is not suitable for the case of liquid-in-tube. The results could be useful for the design of better optofluidic devices based on rolled-up microtubes.

Acknowledgements

This work was supported by the 973 Program (No. 2012CB921604 and 2011CB922004), the NSFC (No. 11004034, 61008029 and 51102049), the Shanghai Pujiang Program (No. 11PJ1400900) and the Program for New Century Excellent Talents in University (No. NCET-10-0345).

References

1 D. Psaltis, S. R. Quake and C. Yang, *Nature*, 2006, **442**, 381–386.
2 C. Monat, P. Domachuk and B. J. Eggleton, *Nat. Photonics*, 2007, **1**, 106–114.
3 V. Ronchi, *Physis*, 1969, **11**, 520–533.
4 W. E. Haas, *Mol. Cryst. Liq. Cryst.*, 1983, **94**, 1–31.
5 L. Dong, A. K. Agarwal, D. J. Beebe and H. Jiang, *Nature*, 2006, **442**, 551–554.
6 X. Heng, D. Erickson, L. R. Baugh, Z. Yaqoob, P. W. Sternberg, D. Psaltis and C. H. Yang, *Lab Chip*, 2006, **6**, 1274–1276.
7 P. Domachuk, H. C. Nguyen, B. J. Eggleton, M. Straub and M. Gu, *Appl. Phys. Lett.*, 2004, **84**, 1838–1840.
8 D. Erickson, T. Rockwood, T. Emery, A. Scherer and D. Psaltis, *Opt. Lett.*, 2006, **31**, 59–61.
9 U. Levy, K. Campbell, A. Groisman, S. Mookherjea and Y. Fainman, *Appl. Phys. Lett.*, 2006, **88**, 111107.
10 E. Chow, A. Grot, W. L. Mirkarimi, M. Sigalas and G. Girolami, *Opt. Lett.*, 2004, **29**, 1093–1095.
11 A. Ksendzov and Y. Lin, *Opt. Lett.*, 2005, **30**, 3344–3346.
12 A. M. Armani and K. J. Vahala, *Opt. Lett.*, 2006, **31**, 1896–1898.
13 D. Yin, D. W. Deamer, H. Schmidt, J. P. Barber and A. Hawkins, *Opt. Lett.*, 2006, **31**, 2136–2138.
14 I. M. White, H. Oveys and X. Fan, *Opt. Lett.*, 2006, **31**, 1319.
15 M. Sumetsky, R. S. Windeler, Y. Dulashko and X. Fan, *Opt. Express*, 2007, **15**, 14376–14381.
16 I. M. White and X. Fan, *Opt. Express*, 2008, **16**, 1020–1028.
17 V. Y. Prinz, V. A. Seleznev, A. K. Gutakovsky, A. V. Chehovskiy, V. V. Preobrazhenskii, M. A. Putyato and T. A. Gavrilova, *Phys. E.*, 2000, **6**, 828.
18 G. Schmidt and K. Eberl, *Nature*, 2001, **410**, 168.
19 Y. Mei, G. Huang, A. A. Solovev, E. Bermudez Urena, I. Monch, F. Ding, T. Reindl, R. K. Y. Fu, P. K. Chu and O. G. Schmidt, *Adv. Mater.*, 2008, **20**, 4085–4090.
20 T. Kipp, H. Welsch, C. Strelow, C. Heyn and D. Heitmann, *Phys. Rev. Lett.*, 2006, **96**, 077403.
21 M. Hosoda and T. Shigaki, *Appl. Phys. Lett.*, 2007, **90**, 181107.
22 C. Strelow, H. Rehberg, C. M. Schultz, H. Welsch, C. Heyn, D. Heitmann and T. Kipp, *Phys. Rev. Lett.*, 2008, **101**, 127403.
23 M. Hosoda, Y. Kishimoto, M. Sato, S. Nashima, K. Kubota, S. Saravanan, P. O. Vaccaro, T. Aida and N. Ohtani, *Appl. Phys. Lett.*, 2003, **83**, 1017.
24 R. Songmuang, A. Rastelli, S. Mendach and O. G. Schmidt, *Appl. Phys. Lett.*, 2007, **90**, 091905.
25 G. Huang, S. Kiravittaya, V. A. Bolanos Quinones, F. Ding, M. Benyoucef, A. Rastelli, Y. F. Mei and O. G. Schmidt, *Appl. Phys. Lett.*, 2009, **94**, 141901.
26 S. Vicknesh, F. Li and Z. Mi, *Appl. Phys. Lett.*, 2009, **94**, 081101.
27 A. Bernardi, S. Kiravittaya, A. Rastelli, R. Songmuang, D. J. Thurmer, M. Benyoucef and O. G. Schmidt, *Appl. Phys. Lett.*, 2008, **93**, 094106.
28 G. Huang, V. A. Bolanos Quinones, F. Ding, S. Kiravittaya, Y. Mei and O. G. Schmidt, *ACS Nano*, 2010, **4**, 3123–3130.
29 E. J. Smith, S. Schulze, S. Kiravittaya, Y. Mei, S. Sanchez and O. G. Schmidt, *Nano Lett.*, 2011, **11**, 4037–4042.
30 X. Fan, I. M. White, S. I. Shopova, H. Zhu, J. D. Suter and Y. Sun, *Anal. Chim. Acta*, 2008, **620**, 8–26.
31 G. Huang, Y. Mei, D. J. Thurmer, E. Coric and O. G. Schmidt, *Lab Chip*, 2009, **9**, 263–268.
32 H. C. van de Hulst, *Light Scattering by Small Particles*, 1981, Dover, New York.
33 X. Hu, C. T. Chan, K. M. Ho and J. Zi, *Phys. Rev. Lett.*, 2011, **106**, 174501.
34 T. Zhan, C. Xu, F. Zhao, Z. Xiong, X. Hu, G. Huang, Y. Mei and J. Zi, *Appl. Phys. Lett.*, 2011, **99**, 211104.
35 Although the Mie theory has been applied to simulate glass capillaries, eqn (3) and (4) have not been presented and only the WGM mode with m = 350 were considered in Ref. 14.

